Structural Monitoring and Maintenance, *Vol. 2, No. 3 (2015) 237-252*
DOI: http://dx.doi.org/10.12989/smm.2015.2.3.237

An experimental study for decentralized damage detection of beam structures using wireless sensor networks

Madhuka Jayawardhana*, Xinqun Zhu[a],
Ranjith Liyanapathirana[b] and Upul Gunawardana[c]

School of Computing, Engineering & Mathematics, University of Western Sydney, Penrith, NSW 2751, Australia

(Received March 8, 2015, Revised August 17, 2015, Accepted August 29, 2015)

Abstract. This paper addresses the issue of reliability and performance in wireless sensor networks (WSN) based structural health monitoring (SHM), particularly with decentralized damage identification techniques. Two decentralized damage identification algorithms, namely, the autoregressive (AR) model based damage index and the Wiener filter method are developed for structural damage detection. The ambient and impact testing have been carried out on the steel beam structure in the laboratory. Seven wireless sensors are installed evenly along the steel beam and seven wired sensor are also installed on the beam to monitor the dynamic responses as comparison. The results showed that wireless measurements performed very much similar to wired measurements in detecting and localizing damages in the steel beam. Therefore, apart from the usual advantages of cost effectiveness, manageability, modularity etc., wireless sensors can be considered a possible substitute for wired sensors in SHM systems.

Keywords: structural health monitoring; decentralized damage detection; wireless sensor networks

1. Introduction

The significance of structural health monitoring (SHM) has been highlighted in the recent years due to the recent catastrophic failures of civil structures (Zhou and Yi 2013). With the advancements of wireless communication technologies and smart devices, wireless sensor networks (WSNs) have rendered the task of SHM more cost effective and convenient as opposed to conventional wired sensor networks, making the deployment of SHM systems practically realisable and manageable (Lynch 2007, Pakzad *et al*. 2008, Ling *et al*. 2009). Wireless sensing technology eliminates the need for laying cables which used to be a tedious and time-consuming task in the case of traditional wired sensor networks. WSNs also reduce the cost involved in installation and maintenance of the system significantly. Thus, WSNs became popular in SHM applications with their modularity, extendibility and manageability. The successful applications of

*Corresponding author, Ph.D., E-mail: m.jayawardhana@uws.edu.au
[a] Ph.D., E-mail: xinqun.zhu@uws.edu.au
[b] Ph.D., E-mail: r.liyanapathirana@uws.edu.au
[c] Ph.D., E-mail: u.gunawardana@uws.edu.au

http://www.techno-press.org/?journal=smm&subpage=7 ISSN: 2288-6605 (Print), 2288-6613 (Online)

WSNs in SHM have exposed many issues related to SHM and these issues have paved the way for many new areas of research. Efficient power management, data communication overheads and optimal sensor configuration are some such issues that have been identified with regard to WSN based SHM systems (Lynch and Loh 2006, Aygun and Gungor 2011, Zhou *et al*. 2014). These have led to developments in many related aspects such as data compression techniques, power management strategies, error recovery algorithms and improved hardware components. Despite the vast amount of existing work in literature (Lynch 2007, Zhou and Yi 2014, Spencer *et al*. 2015), the use of WSNs in SHM can still be a challenging task. As mentioned before, limited energy in wireless sensors is a major contributor for these challenges (Anastasi *et al.* 2009).

Decentralized data processing is one such solution that is being investigated for its potential in energy saving of sensors and data reduction (Gao *et al.* 2006, Jindal and Liu 2012, Liu *et al*. 2014). In traditional SHM systems, the damage identification techniques are centralized, in the sense that, all sensor nodes collect the data and transmit them to a central location to be processed which is ultimately responsible for the damage decision making. It is not feasible to stream the raw data back to the server due to the low bandwidth and energy limitations of low-power wireless sensor networks. Decentralized damage detection is processing the structural response data in each sensor node itself partly or fully, and the partially processed data or the arrived decision is sent to the central node. It is said that transmitting one bit through wireless communication may consume as much energy as executing a few thousands instructions in a processor (Meo and Zumpano 2005, Pottie *et al.* 2008). Considering this fact, by vastly reducing the amount of wireless communication and the transmitted data amount, decentralized methods consume much less energy compared to centralized methods making the battery power of the SHM system last longer. Because the data amount to be transmitted is considerably decreased in decentralized methods, the sampling rate as well as the node density can be significantly increased (Liu *et al.* 2009). Due to the computing environment offered by WSNs is highly decentralized with a large number of lightweight computing nodes, decentralized structural damage detection has a high potential for development. Lynch *et al*. (2006) first proposed the concept of decentralized computing for modal parameter identification. Zimmerman *et al*. (2008) presented a parallel computing paradigm to embed the frequency-domain decomposition method in the wireless sensor network for automated mode shape extraction. Kim and Lynch (2012) proposed a decentralized system identification method based on Markov parameters. Hackmann *et al*. (2012, 2014) adopted the damage localisation assurance criterion algorithm to implement the decentralized structural damage localisation. From the above, the decentralized data processing has the benefit of improving wireless monitoring system scalability, reducing the amount of wireless communications, and reducing overall power consumption.

This paper presents a comparative study carried out using wired and wireless sensor data for effective structural damage identification. Two decentralized damage identification methods developed in the authors' previous work are used in this analysis for damage detection and localisation. One is the damage index based on the Auto-regressive model (ARD) which is a statistical time-series method based on the auto regressive (AR) model (Jayawardhana *et al*. 2011). A novel approach for decentralized damage identification, based on the Wiener filter is the second method (Jayawardhana *et al*. 2013). Experimental data from a series of tests carried out on a steel beam equipped with wired and wireless sensor networks were used for the comparison study. Comparison of the identified results using ambient and impact testing is also presented along with the ARD and Wiener filter method analysis. The observations from the results are discussed before presenting the conclusions from the analysis.

2. Decentralised damage detection methods

Two decentralized damage identification methods were used for this analysis, namely - the ARD method (Jayawardhana *et al.* 2011) and the Wiener filter method (Jayawardhana *et al*. 2013). These two methods would be introduced briefly in the section.

2.1 ARD method

The ARD method is a statistical time-series based structural damage detection method which makes use of the Auto-regressive model. The coefficients from the AR models fitted to structural responses from the reference state of the structure and those from the unknown state of the structure are used to compute a damage sensitive feature (DSF) named D index which is used for damage detection. The structural responses are normalised before they are used to fit the AR model. This D index is represented as

$$D = \sum_{i=1}^{p} (\phi_i^y - \phi_i^x)^2 \tag{1}$$

where p is the AR model order and ϕ_i^y, ϕ_i^x are the AR model coefficients of the current data y (from unknown state of the structure) and reference data x respectively. The AR model order p is determined by exploring the autocorrelation function of the model residual errors (Box *et al.* 2013).

A reference D index set (D_{ref}) is setup as the reference database. The current D index set (D_{curr}) is calculated by comparing the AR model coefficients of the current state data and the reference data set. The current damage index D_{curr} is compared against the reference database in each sensor for damage decision making. This damage identification process will be carried out in each sensor node. The threshold is determined by the statistical analysis with a confidence level of 99% in a normal distribution populated by the D indices' probability density function. Two threshold values are calculated for each sensor as follows

$$Thr = \mu_{ref} \pm 3\sigma_{ref} \tag{2}$$

where μ_{ref}, σ_{ref} are the means and variances of D indices from the reference data respectively.

The Fisher criterion f is computed for each sensor using the above D indices.

$$f = \frac{(\mu_{curr} - \mu_{ref})^2}{\sigma_{curr}^2 - \sigma_{ref}^2} \tag{3}$$

where $\mu_{curr}, \sigma_{curr}$ are the means and variances of D indices from the current state respectively. The calculated Fisher criteria values of all sensors will be transmitted to the central station for comparison to determine the damage location. The damage identification algorithm is carried out in a decentralised manner. The data processing is executed in the individual sensors and only the

Fisher criterion values in each sensor are transmitted to the central station for damage localisation. The values are calculated in the individual sensors and there are no synchronization sampling requirement in this algorithm.

2.2 Wiener filter technique

The Wiener filter method is proposed for decentralized damage identification. The mean square error (MSE) value of the optimum Wiener filter constructed from structural responses is used as the damage detection index (DDI). This DDI is represented in terms of the optimum Wiener filter error $e(n)$ as

$$DDI = E[e^2(n)] \tag{4}$$

where the Wiener filter error $e(n) = d(n) - y(n)$ with $d(n)$ as an estimation of the desired signal and $y(n)$ as the resulting noise-reduced filter output which is targeted to be an estimation of $d(n)$, respectively.

The proposed method involves two phases, namely damage detection and localisation. In the first phase damage detection is carried out locally and independently in each wireless sensor node using the MSE of the Wiener filter from measured responses. This in-node data processing and decision making brings the concept of decentralized damage detection into the method. The threshold is determined by statistical analysis with a 99% confidence level. The current DDI values are calculated using current measurements and compared with the reference DDI values stored in each sensor for structural damage detection. In the damage localisation phase, sensors are paired off for damage localisation. The cross correlation coefficients of the DDI values from sensor pairs are computed and the variances of these coefficients are used for damage localisation. As the data processing is carried out in each sensor node or between two sensor nodes, the synchronization error does not have a big effect on the result. The process is carried out in the central station.

3. Experimental study

Experimental data from a series of excitation tests carried out on a steel beam structure are used in this study. Fig. 1 shows an overall representation of the experimental setup. Both wired and wireless sensors were installed in the selected test specimen appropriately. Measurements from these sensors were collected by the means of two laptop computers and aggregated at a central computer - referred to as the central server in this paper - for processing. Wired sensors were connected to the laptop computer via the necessary power supply and data hub setup, and the wireless sensor measurements were acquired via a base station. The measurements were obtained from two types of structural excitation tests; impact test and ambient test. Further, damage detection algorithms require both reference state measurements and damaged state measurements of the structure for their verification. Thus, undamaged structure's responses were acquired initially from the structure as the reference state measurements before creating damages in the structure for damaged state measurements. The experimental setup and the procedure are described in detail in the following sections.

3.1 Experimental setup

A steel beam was selected as the test specimen with the aim of detecting structural damage in more localized damage scenarios as that will demand better accuracy in damage localisation. A 4 m long 100UC14.8 steel beam as shown in Fig. 2 was used as the test specimen. The density of the beam is $14.8\,kg/m$ and the Young's modulus E is $200\times10^{9}\,N/m^{2}$. Two concrete blocks of dimensions $60\,mm\times60\,mm\times238\,mm$ were used to support the beam, placed with an over-hang of 100mm from each end as shown in Fig. 2(a). Fig. 2(b) shows the location of the sensors. Seven sensor locations are uniformly distributed along the axis of the beam. The impact point shown in Fig. 2(b) is where the impact force was applied.

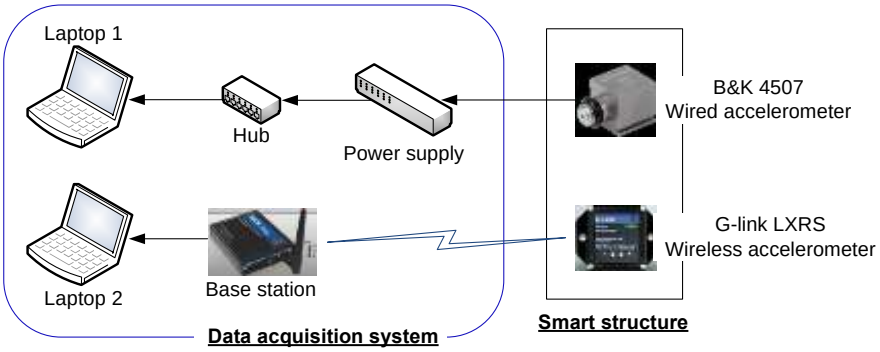

Fig. 1 An overall view of the experimental setup

(a) Beam setup

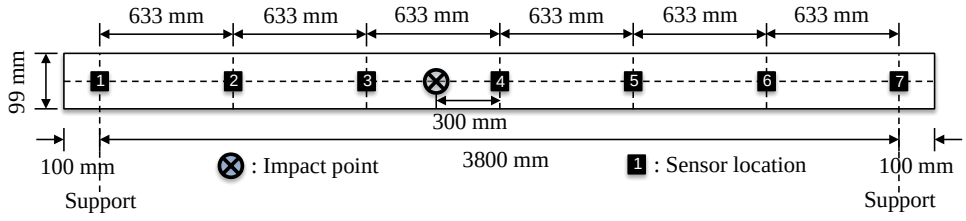

(b) Sensor locations

Fig. 2 Experimental setup and sensor locations

The data acquisition process was carried out using both wireless and wired sensors. The wireless sensor network of the data acquisition system consists of seven Microstrain G-link-LXRS wireless accelerometer nodes. The frequency bandwidth of the nodes is 0 Hz to 500 Hz and the accuracy is 10 mg. These sensors were installed on the steel beam uniformly distributed between the two supports along the beam's longitudinal axis. A Microstrain WSDA-104 base station was used to acquire data from the G-link wireless accelerometers. The wired sensor network of the data acquisition system consisted of seven Brüel & Kjær 4507 piezoelectric accelerometers. The frequency range of these accelerometers is 0.3~6000 Hz and the sensitivity is 1000 mV/g. These sensors were installed along the beam just next to the wireless sensors as shown in Fig. 2(a).

Fig. 3 shows the impulse responses of the structure obtained using both wired and wireless sensors. From this figure it is evident that the wireless sensor impulse response is very much similar to the wired sensor impulse response in magnitude. Frequency spectra of the two responses illustrated in Fig. 3(b) also show similarity, but there are some difference in spectrum. This is due to the frequency range and sensitivity of wireless sensors are different with that of wired sensors.

3.2 Damage scenarios

In order to verify two algorithms, seven different damage states were simulated in the steel beam. Damages were created in the beam by cutting the bottom flange of the beam using an angle grinder with different depths in two different locations. The depth is the average value of three different measurements after the beam has been cut. The details of these damage scenarios are illustrated in Table 1. D11 to D13 represents the first three damage scenarios carried out by increasing the depth of the cut at one location, that is 850mm from the left support. For Damage scenario D13 the complete bottom flange was removed with a width of 3mm. For Damage scenarios D21 to D24, another cut at 2400 mm from the left support with different depths is added. Although D21 to D23 vary by the increasing depth of the cut, D24 differs from the other scenarios by the increased width of the cut as shown in Table 1.

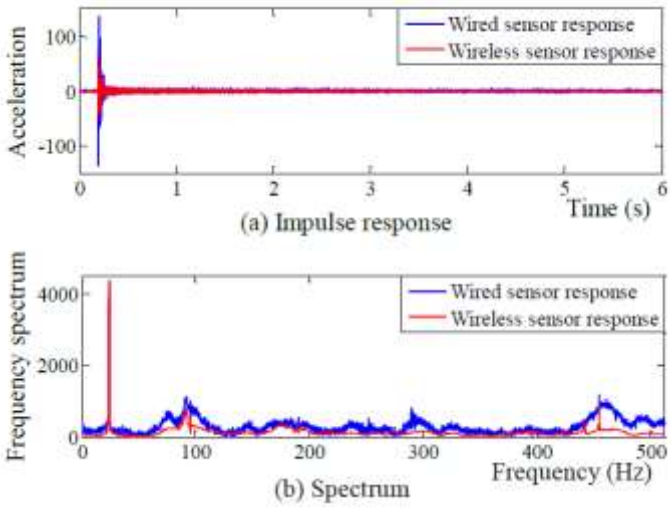

Fig. 3 The impulse response of the structure measured using wired and wireless sensors

Table 1 Details of damage scenarios

Damage Scenario	D11	D12	D13	D21	D22	D23	D24
Distance from left support (mm)	850	850	850	2400	2400	2400	2400
Distance from left corner (mm)	950	950	950	2500	2500	2500	2500
Depth of the cut (mm)	16.5	33	49.5	16.5	33	49.5	49.5
Width of the cut (mm)	3	3	3	3	3	3	30

Note: The depth is the avergae of three different measurements at the cut

3.3 Experimental procedure

Four sets of measurements were obtained from the test structure in each scenario from two types of tests, the impact and ambient testing. Impact responses of the structure were obtained by impact tests performed using the instrumented impact hammer. The frequency range with the hard tip is 0~1 kHz and the sensitivity is 0.23 mV/N. Ambient responses of the structure were also obtained considering the environmental excitation to the structure. Since wired and wireless sensor measurements are acquired in both these tests, four sets of structural measurements are collected from this experiment:

- impact responses from wired sensors
- impact responses from wireless sensors
- ambient responses from wired sensors
- ambient responses from wireless sensors

Before creating any of the damage scenarios in Table 1, reference acceleration responses (undamaged responses) of the beam were collected from both ambient and impact tests. The damages were simulated one by one on the beam by cutting the bottom flange of the beam using the angle grinder. The ambient and impact tests were carried out for each damage scenario.

A sampling rate of 1024Hz was used in all the measurements. The data length of each record is 6144, which amounts to 6 seconds to capture the whole response. Ambient responses were obtained for approximately 10 minutes making each record length approximately 614400. 10 impact tests and four ambient tests were obtained in each scenario.

4. Results and discussion

Dynamic response measurements on the steel beam structure were used to analyse the performance and reliability of wireless sensors for SHM as opposed to wired sensors. Two decentralized damage identification methods listed in Section 2 were used for this analysis. A comparison between impact responses and ambient responses will also be carried out. The following sections present the results and the discussion that follows on the aforementioned studies.

4.1 Impact testing results

4.1.1 Damage detection using the ARD and Wiener filter methods

Impact responses from wired and wireless sensors will be used for structural damage detection in this section. Two damage indices, the D-index in the ARD method and the MSE value in the Wiener filter method, are used to indicate the damage in the structure. Since all the sensors presented similar results for structural damage detection, only the results at Sensor 2 are listed here, chosen arbitrarily. 10 impact tests were performed in each scenario giving 10 impact response samples and 100 damage index values were obtained in the damage detection process by pairing each sample from the damaged state with one of the 10 reference samples. Fig. 4 presents the D index values from wired and wireless measurements at Sensor 2 with different damage in the beam. The difference between D index values from wired and wireless measurements is due to the available wired and wireless sensors have different frequency ranges and sensitivities. The D index is calculated by Eq. (1) and the result is a relative value. In the figure, the D index values from all damage scenarios are much higher than those from the reference one and there is a clear gap between the damage states and the reference one. From these results, it is quite clear that damage is successfully indicated by the D-index using the ARD method from both wired and wireless measurements. Similar to the ARD method, the 100 MSE values are also obtained by Eq. (3) as shown in Fig. 5. The similar observation to the ARD method can be obtained from these results. The results from wired measurements are much clearer than that from wireless measurements. This is because the local damage is sensitive to the high frequency component. Compared the wireless sensors, the wired sensor is much sensitive to the high frequency response component.

4.1.2 Damage localisation using the ARD and Wiener filter methods

In the ARD method, the Fisher criterions are calculated using Eq. (2) to detect the location of the damage. Figs. 6(a)-6(c) show the results from wired measurements on the beam with damage scenarios D13, D21 and D24 respectively. In Fig. 6(a), the Fisher criterion value at Sensor 2 is much higher than that at other sensor locations. As listed in Table 1, the damage location for D13 is close to Sensor 2 and the damage location is correctly detected. The smaller peak at Sensor 6 is an outlier caused by the symmetry of the structure. Fig. 6(b) shows that two damage locations are identified by a large peak at Sensor 2 and a smaller peak at Sensor 5. These confirm the correct damage localisation of damage scenario D21 in which, a larger damage close to Sensor 2 and a smaller damage between Sensors 4 and 5 had taken place. Similarly, in Fig. 6(c) the two damages are identified: one at Sensor 2 and another one at Sensor 5 by two peaks. Also almost all of the sensors have shown considerably higher values which may be accounted to the high severity of damage at this damage scenario.

Fig. 7 shows the results using wireless measurements. Similar to the results from the wired measurements, the Fisher criterions for damage scenarios D13, D21 and D24 are plotted in Figs. 7(a)-7(c) respectively. In Fig. 7(a) there is a peak value at Sensor 2 indicating damage location. In Fig. 7(b) there are two peaks, one at Sensor 2 and another one at Sensors 4 and 5, which are corresponded to two damage locations of D21. There is a peak at Sensor 7 and this is due to the measurement noise. As the response at the support is very small, the signal-to-noise ratio is also very low. The noise will induce a large Fisher criterion value from Eq. (2) as it is a relative value. In Fig. 6(c) there are two peaks around Sensors 2 and 5, respectively. The results show that the damage locations are around Sensors 2 and 5.

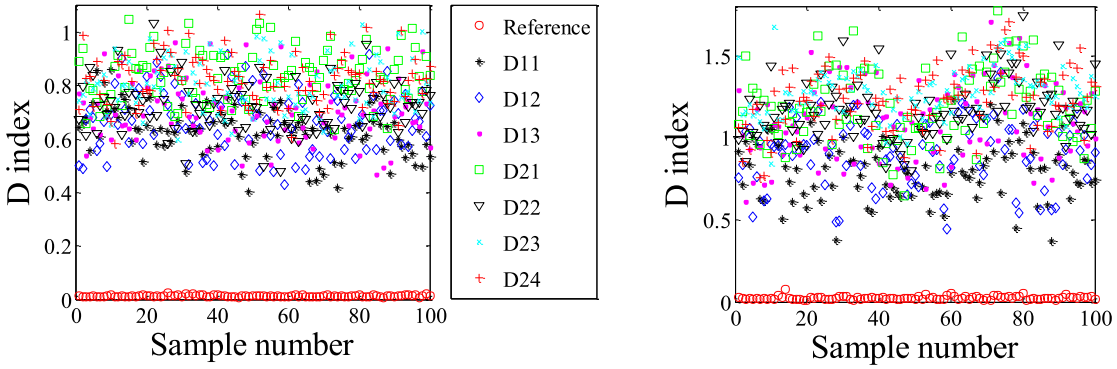

(a) from wired measurements (b) from wireless measurements

Fig. 4 Damage detection with ARD method using wired and wireless measurements

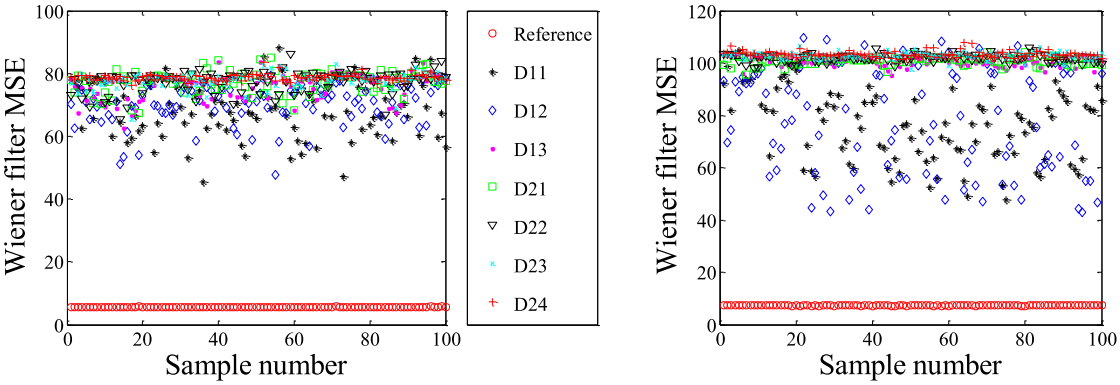

(a) Wired measurements (b) Wireless measurements

Fig. 5 Damage detection with the Wiener filter method using wired and wireless measurements

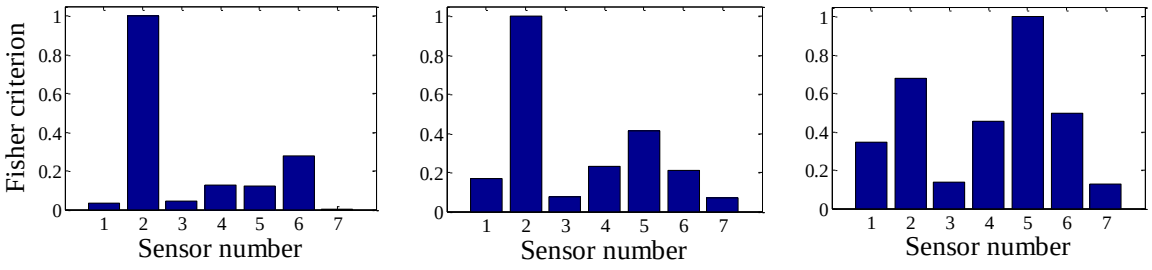

(a) D13 (b) D21 (c) D24

Fig. 6 Damage localisation with ARD method, using wired impact responses measurements

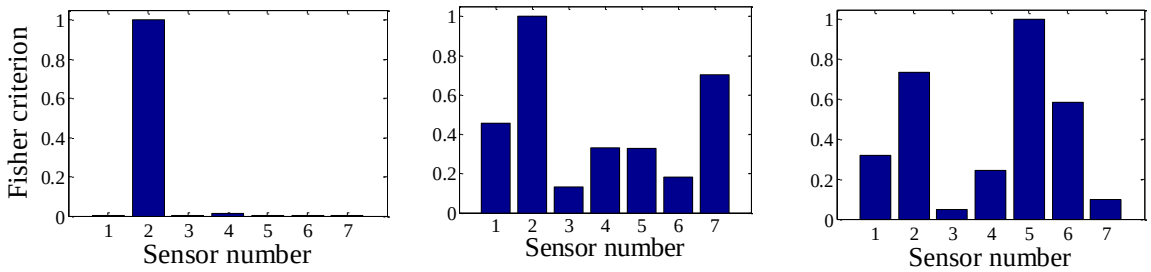

(a) D13 (b) D21 (c) D24

Fig. 7 Damage localisation with the ARD method, using wireless impact responses

In the Wiener filter method, the damage localisation is obtained by pairing the sensors to gain the spatial information of the damage. As the sensors are placed uniformly along the beam, nearby sensors are paired off for damage localisation. There are seven sensors and each sensor is paired with its two neighbour sensors making 6 pairs of sensors, for example Sensors 1 and 2, Sensors 2 and 3 etc. The Wiener filter MSE value from the two sensors of a sensor pair are used to calculate the cross correlation coefficients. The damage localisation index (DLI) is determined by the statistical variation of these coefficients (Jayawardhana *et al.* 2013). As the results from wired measurements are similar to that by wireless measurements from the above, only the results by wireless measurements are listed here, as shown in Fig. 8. In Fig. 8(a), the DLI values for Sensor pairs 1 and 2 are much higher than others. Sensor 2 is the common sensor for Sensor pairs 1 and 2 and the damage location will be around Sensor 2. Fig. 8(b) shows the high values at Sensor pairs 2 and 5 that are related to one damage between Sensors 2 and 3, and another damage between Sensors 4 and 5. Fig. 8(c) shows that there are two peaks, one is around Sensor pairs 1 and 2, and another one is around Sensor pair 5. The results successfully indicated the damage locations around Sensors 2 and 5. Damage localisation performance using the impulse responses with the Wiener filter method seem to be similar between wired and wireless sensors.

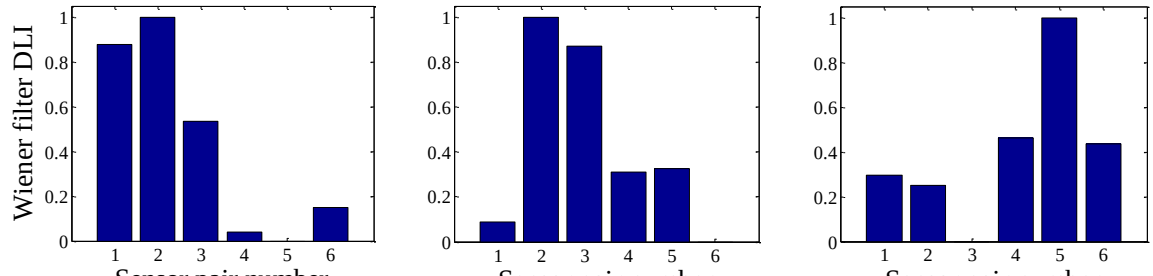

(a) D13 (b) D21 (c) D24

Fig. 8 Damage localisation with the Wiener filter method using wireless measurements

4.1.3 Damage severity estimation using the ARD and Wiener filter methods

A basic damage quantification analysis has also been carried out using the mean of the D index. The mean D indices from different damage scenarios D11 to D24 are plotted in Fig. 9. Fig. 9(a) shows the mean D index increases with the damage intensity in general. This provides a general understanding of the intensity of damages in the experiment. The value at D21 has a high value because the second damage is added at this damage scenario and there is a big change between D13 and D21. Compared to the wired results, Fig. 9(b) shows that there is an approximate linear relationship between the mean D index and the damage severity. The similar results are obtained using the Wiener filter method as shown in Fig. 10.

In general, both the ARD method and the Wiener filter method are successful in structural damage detection, localisation and basic quantification of damage using both wired and wireless impact responses from the experiment. It was also seen that wired and wireless sensors have performed equally well in this analysis. Compared to this situation, damage localisation using the ARD method were much clear. Nevertheless, utilisation of structure's spatial information in the Wiener filter method can be advantageous in larger structures as it will provide more information on the damage location, making the process easier.

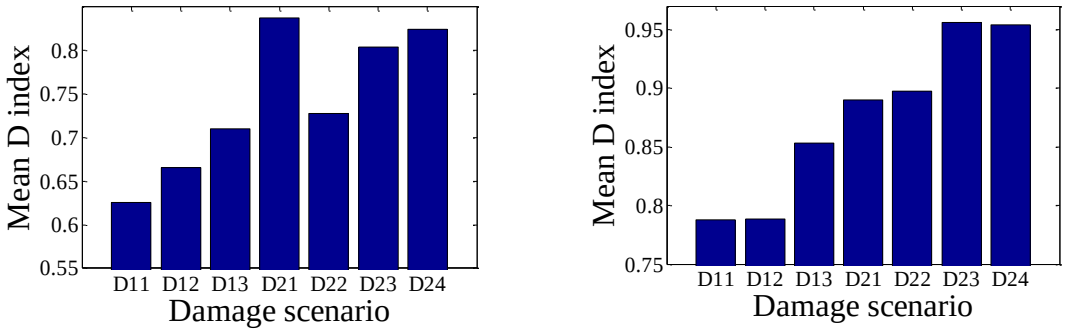

(a) Wired measurements (b) Wireless measurements

Fig. 9 Damage quantification with ARD method, using wired and wireless impact responses

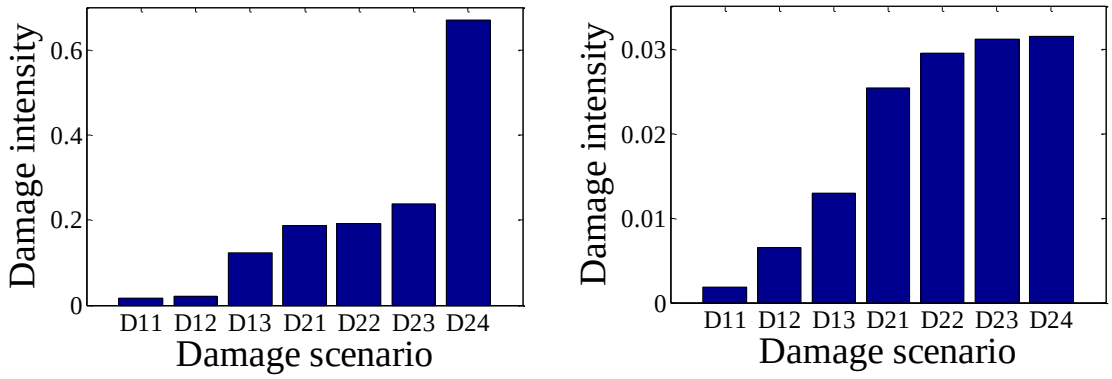

(a) Wired measurements (b) Wireless measurements

Fig. 10 Damage quantification with Wiener method using wired and wireless measurements

4.2 Ambient testing

4.2.1 Damage detection using the ARD and Wiener filter methods

This section focuses on the structural damage identification using the ambient testing. As a single record of ambient responses was about 614400 in length from both wired and wireless sensors, these records were split into segments of length 6144 for convenience in computations. Approximately 100 data samples resulted in this segmentation.

Fig. 11 shows the damage detection results using the segmented ambient response samples. D indices computed from wired and wireless measurements of all damage scenarios are presented in Figs. 11(a) and 11(b) respectively. A clear difference between the damaged D indices and reference D indices are shown in both these two figures. This indicates correct damage detection in all damage scenarios using ambient measurements.

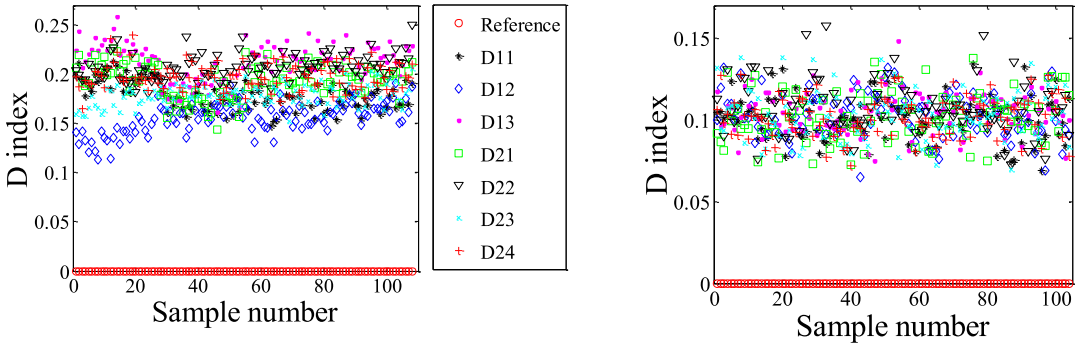

(a) Wired measurements (b) Wireless measurements

Fig. 11 Damage detection with ARD method, using wired and wireless ambient responses

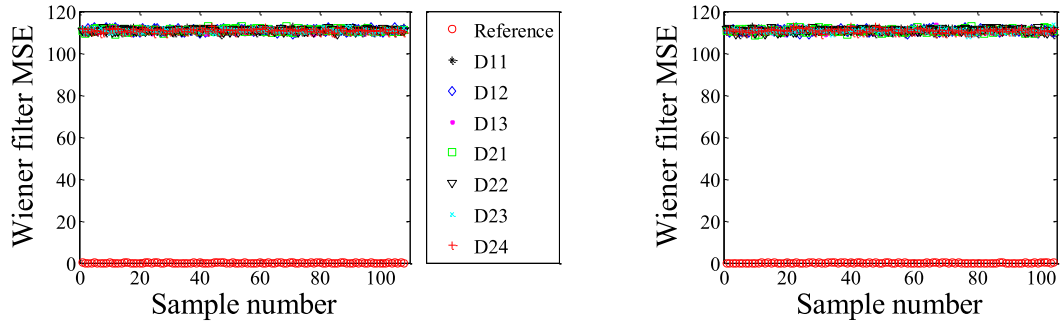

(a) Wired measurements (b) Wireless measurements

Fig. 12 Damage detection with the Wiener filter method, using wired and wireless ambient responses

Fig. 12 illustrates the damage detection results obtained from the ambient responses of wired and wireless sensors through the Wiener filter method. The results show that there is a clear gap between the MSE values from all the damage scenarios and the reference state. This indicates successful damage detection with a good confidence margin from ambient measurements. It evident that wireless sensors have performed equally well as wired sensors in this damage detection process using the Wiener filter method.

4.2.2 Damage localisation using the ARD and Wiener filter methods

Damage localisation results from damage scenarios D13 and D21 of the wired ambient responses are illustrated in Figs. 13(a) and 13(b) respectively. Fig. 13(a) shows a peak value at Sensor 2 and comparatively smaller values at Sensors 4, 5 and 6. The peak at Sensor 2 is a result of damage, which is close to Sensor 2. However, Sensors 4, 5 and 6 have shown faulty results due to the measurement noise. Fig. 13(b) shows correct localisation of the first damage at Sensor 2 as well as the second damage at Sensors 4 and 5. The peak value at Sensor 6 can be accounted to the sensitivity of Sensor 6 to the effects of the second damage which is closer to Sensor 5 rather than Sensor 4. Fig. 13(c) presents two peak values: one at Sensor 2 and the second one at Sensor 5. Thus the damage localisation of D24 is successful.

The results using wireless measurements are illustrated in Fig. 14. In Fig. 14(a) there is a peak value at Sensor 2 that is the damage location for damage scenario D13. Fig. 14(b) has located the first damage at Sensor 2, and the second damage at Sensors 4 and 5 correctly from D21 damage scenario. Fig. 14(c) has shown correct localisation of the first damage at Sensors 2 and 3. However, the localisation of the second damage is not so accurate as it has actually occurred between Sensors 4 and 5 instead of nearer to Sensor 6 as shown in the figure. Therefore, compared to the results from wireless responses, ARD damage localisation has performed slightly better with the wired responses.

Fig. 15 shows the localisation results of wireless ambient responses using the Wiener filter method. Fig. 15(a) presenting the localisation of damage scenario D13 has located the first damage accurately at sensor pair 2, with an erroneous peak at Sensor pair 6 due to the measurement error at Sensor 7 (the support). The first damage is accurately localised in Sensor pair 2 in Fig. 15(b) - which presents the D21 damage scenario - with additional peaks at Sensor pairs 1 and 3 caused by the close proximity of damage as described previously. The second damage is located at Sensor 5 picked up by sensor pair 5. Similar results are observed in Fig. 15(c) where the first damage is located by Sensor pairs 1 and 2 and the second damage by sensor pair 5 correctly.

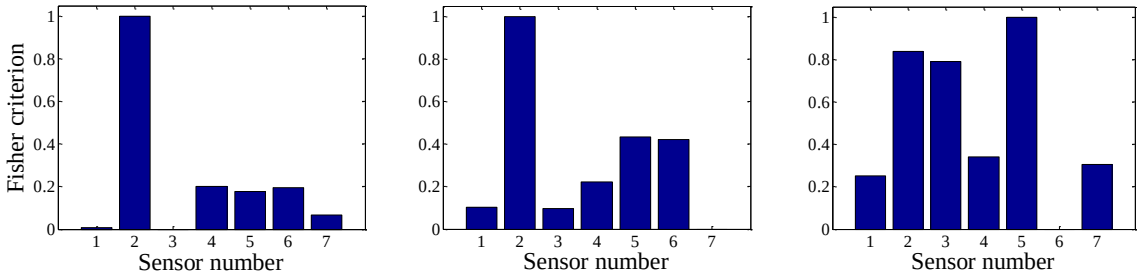

(a) D13 (b) D21 (c) D24

Fig. 13 Damage localisation with the ARD method, using wired ambient responses

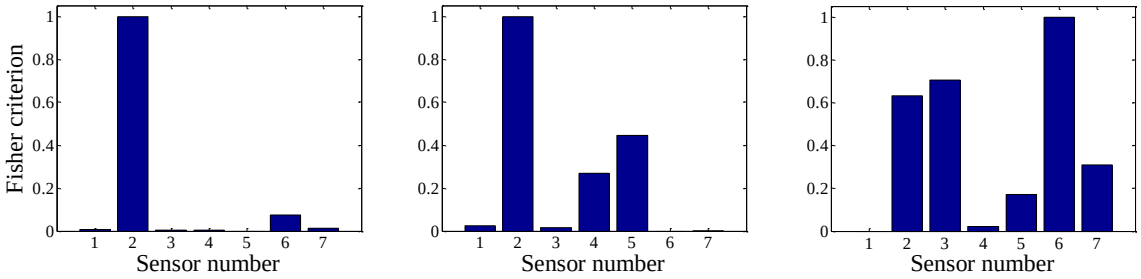

(a) D13 (b) D21 (c) D24

Fig. 14 Damage localisation with the ARD method, using wireless ambient responses

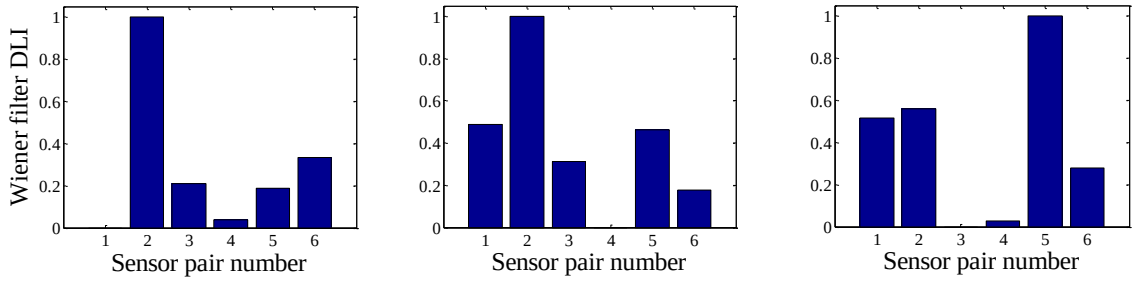

(a) D13 (b) D21 (c) D24

Fig. 15 Damage localisation with the Wiener filter method, using wireless ambient responses

4.2.3 Damage severity estimation using the ARD and Wiener filter methods

Results from a comparative damage quantification using the mean D index and Damage intensity are illustrated in Fig. 16. In Fig. 16(a), the mean value of the D index values increases with the damage severity. The values from damage scenarios with two damages are much larger than that with single damage. Fig. 16(b) shows the results using the Wiener filter method. The results show an increase of the value with damage severity. Further study is needed to accurate quantify the damage severity, especially from ambient measurements.

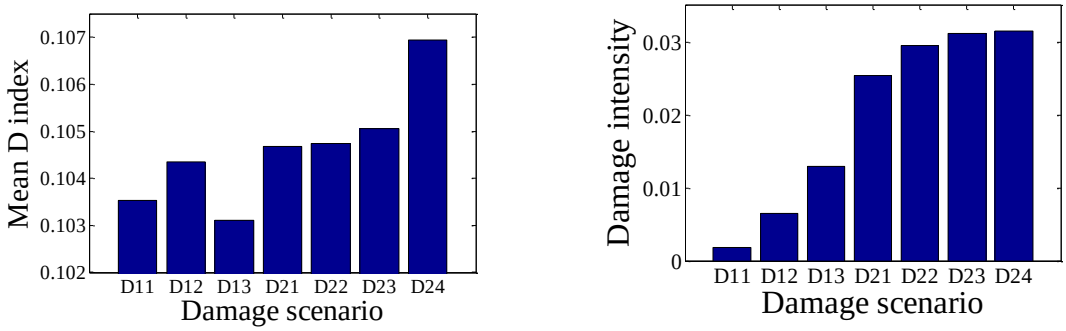

(a) The ARD method (b) The Wiener filter method

Fig. 16 Damage severity estimation using wireless ambient responses

5. Conclusions

An experimental study for decentralized damage detection using wireless sensor networks has been carried out. Experimental data from a series of tests carried out on a steel beam equipped with the wireless and wired sensor networks were used as a comparison study. The two recently developed decentralized damage detection algorithms were verified for performance and reliability. Both impact and ambient testing were carried out to examine these two methods in the laboratory.

The wireless sensors provided similar results to the wired sensors and enabled a similar level of structural damage to be identified. The possibility of using wireless sensors in SHM systems thus appears to be a viable opportunity. The effectiveness of the decentralized algorithms was also successfully examined in their application to the detection and localisation of damage. Future work will include applying these damage detection algorithms in wireless sensors to enable real-time monitoring of structures.

Acknowledgments

The authors gratefully acknowledge the financial support provided by the Research Grants Scheme of University of Western Sydney.

References

Anastasi, G., Conti, M., Di Francesco, M. and Passarella A. (2009), "Energy conservation in wireless sensor networks: A survey", *Ad Hoc Networks*, **7**(3), 537-568.

Aygun, B. and Gungor, V.C. (2011), "Wireless sensor networks for structural health monitoring: recent advances and future research directions", *Sensor Rev.*, **31**(3), 261-276.

Box, G.E., Jenkins, G.M. and Reinsel, G.C. (2013), *Time Series Analysis: Forecasting and Control*, Wiley. com.

Gao, Y., Spencer, B.F. and Ruiz-Sandoval, M. (2006), "Distributed computing strategy for structural health monitoring", *Struct. Control Health Monit.*, **13**(1), 488-507.

Hackmann, G., Guo, W., Yan, G., Sun, Z., Lu, C. and Dyke, S. (2014), "Cyber-physical co-design of distributed structural health monitoring with wireless sensor networks", *IEEE T. Parall. Distr.*, **25**(1), 63-72.

Hackmann, G., Sun, F., Castaneda, N., Lu, C. and Dyke, S. (2012), "A holistic approach to decentralized structural damage localization using wireless sensor networks", *Comput. Commun.*, **36**(1), 29-41.

Jayawardhana, M., Zhu, X.Q. and Liyanapathirana, R. (2011), "Structural damage detection of RC structures using AR model coefficients", *Proceedings of the 14th Asia Pacific Vibration Conference*, December 2011, Hong Kong.

Jayawardhana, M., Zhu, X.Q. and Liyanapathirana, R. (2013), "Decentralized damage detection of RC structures using the Wiener filter", *Australian J. Struct. Eng.*, **14**(1), 57-69.

Jindal, A. and Liu, M. (2012), "Networked computing in wireless sensor networks for structural health monitoring", *IEEE/ACM T. Networking*, **20**(4), 1203-1216.

Kim, J. and Lynch, J. (2012), "Autonomous decentralized system identification by Markov parameter estimation using distributed smart wireless sensor networks", *J. Eng. Mech. - ASCE*, **138**(5), 478-490.

Ling, Q., Tian, Z., Yin, Y. and Li, Y. (2009), "Localized structural health monitoring using energy-efficient wireless sensor networks", *IEEE Sens. J.*, **9**(11), 1596-1604.

Liu, X., Cao, J., Xu, Y., Wu, H. and Liu Y. (2009), "A multi-scale strategy in wireless sensor networks for

structural health monitoring", *Proceedings of the 5th International Conference on Intelligent Sensors, Sensor Networks and Information Processing (ISSNIP).*

Lynch, J.P. and Loh, K.J. (2006), "A summary review of wireless sensors and sensor networks for structural health monitoring", *Shock Vib. Digest*, **38**(2), 91-130.

Lynch, J.P. (2007), "An overview of wireless structural health monitoring for civil structures", *Philos. T. R. Soc. A*, **365**(1851), 345-372.

Meo, M. and Zumpano, G. (2005), "On the optimal sensor placement techniques for a bridge structure", *Eng. Struct.*, **27**(10), 1488-1497.

Pakzad, S., Fenves, G., Kim, S. and Culler, D. (2008), "Design and implementation of scalable wireless sensor network for structural monitoring", *J. Infrastruct. Syst. - ASCE*, **14**(1), 89-101.

Pottie, G.J. and Kaiser, W.J. (2000), "Wireless integrated network sensors", *Communications of the ACM*, **43**(5), 51-58.

Spencer, B.F., Jo, H., Mechitov, K.A., Li, J., Sim, S.H., Kim, R.E., Cho, S., Linderman, L.E., Moinzadeh, P., Giles, R.K. and Agha, G. (2015), "Recent advances in wireless smart sensors for multi-scale monitoring and control of civil infrastructure", *J. Civil Struct. Health Monit.*, DOI 10.1007/s13349-015-0111-1.

Zhou, G.D. and Yi, T.H. (2013), "Recent developments on wireless sensor networks technology for bridge health monitoring", *Mathematical Problems in Engineering*, Article ID 947867, http://dx.doi.org/10.1155/2013/947867.

Zhou, G.D., Yi, T.H., Zhang, H. and Li, H.N. (2014), "Energy-aware wireless sensor placement in structural health monitoring using hybrid discrete firefly algorithm", *Struct. Control Health Monit.*, DOI: 10.1002/stc.1707.

Zimmerman, A.T., Shiraishi, M., Swartz, R.A. and Lynch, J.P. (2008), "Automated modal parameter estimation by parallel processing within wireless monitoring systems", *J. Infrastruct. Syst. - ASCE*, **14**(1), 102-113.